Recombinant inbred line panels inform the genetic architecture and interactions of adaptive traits in *Drosophila melanogaster*

Authors: Tiago da Silva Ribeiro[1,2,a,@], Matthew J. Lollar[1], Quentin D. Sprengelmeyer[1b], Yuheng Huang[1c], Derek M. Benson[1], Megan S. Orr[1], Zachary C. Johnson[1], Russell B. Corbett-Detig[3,4], John E. Pool[1,2,@]

Mailing address:

[1] Laboratory of Genetics, University of Wisconsin-Madison, Madison, WI, 53706, USA

[2] Department of Integrative Biology, University of Wisconsin-Madison, Madison, WI, 53706, USA

3. Genomics Institute, University of California, Santa Cruz, Santa Cruz, CA, 95064, USA

4. Department of Biomolecular Engineering, University of California, Santa Cruz, Santa Cruz, CA, 95064, USA

[a] Current address: Instituto de Biociências, Universidade de São Paulo, São Paulo, Brazil, 05508-090.

[b] Current address: Department of Equity and Inclusion, University of Wisconsin-Platteville, Platteville, WI, 53818

[c] Current address: Department of Ecology and Evolutionary Biology, University of California, Irvine, Irvine, CA, 92697.

[@] Corresponding authors:

Tiago da Silva Ribeiro, tribeiro@wisc.edu

John E. Pool, jpool@wisc.edu

Keywords: epistasis, Quantitative Trait Loci (QTL), adaptation, quantitative genetics, *Drosophila melanogaster*.

Abstract

The distribution of allelic effects on traits, along with their gene-by-gene and gene-by-environment interactions, contributes to the phenotypes available for selection and the trajectories of adaptive variants. Nonetheless, uncertainty persists regarding the effect sizes underlying adaptations and the importance of genetic interactions. Herein, we aimed to investigate the genetic architecture and the epistatic and environmental interactions involving loci that contribute to multiple adaptive traits using two new panels of *Drosophila melanogaster* recombinant inbred lines (RILs). To better fit our data, we re-implemented functions from R/qtl (Broman *et al*. 2003) using additive genetic models. We found 14 quantitative trait loci (QTL) underlying melanism, wing size, song pattern, and ethanol resistance. By combining our mapping results with population genetic statistics, we identified potential new genes related to these traits. None of the detected QTLs showed clear evidence of epistasis, and our power analysis indicated that we should have seen at least one significant interaction if sign epistasis or strong positive epistasis played a pervasive role in trait evolution. In contrast, we did find roles for gene-by-environment interactions involving pigmentation traits. Overall, our data suggest that the genetic architecture of adaptive traits often involves alleles of detectable effect, that strong epistasis does not always play a role in adaptation, and that environmental interactions can modulate the effect size of adaptive alleles.

Introduction

Adaptive evolution is the result of natural selection, which acts by increasing the frequency of beneficial traits in a population. A number of important uncertainties persist regarding the genetic architectures of adaptive trait changes in nature, including the number and effect sizes of contributing variants, and their frequencies before and after the action of positive selection (Pritchard *et al*. 2010, Savoleinen *et al*. 2013, Barghi *et al*. 2020). Furthermore, research on the genetic basis of adaptation has largely been centered on the individual additive effects of each gene underlying the adaptive trait, whereas the role of gene-by-gene and gene-by-environment interactions in adaptation has remained more elusive (Whitlock *et al*. 1995, Malmberg & Mauricio 2005, Martin & Lenormand 2006, Bank 2022).

Theoretical and empirical studies have yielded varied findings concerning the number and strength of loci contributing to adaptive trait change. Fisher (1930) argued that traits were governed by numerous genetic variants of very small magnitude, and that natural selection proceeded via minute incremental changes in allele frequency at these loci. Extending Fisher's geometric model, Orr (1998) found that in a sequential model of genetic adaptation, a few larger effect sizes should tend to be followed by many smaller ones, yielding an exponential distribution of effects. However, adaptation in natural populations may sometimes depart from the assumptions of such models in multiple respects. First, the role of standing variation (as opposed to new mutations) in the adaptive process continues to be investigated (Fuhrmann *et al*. 2023, Schlötterer 2023), and these two sources of genetic variation may differ in their effect sizes, dominance, and other properties (e.g. Orr & Betancourt 2001). Second, the genetic architecture of local

70 adaptation, in which populations in a heterogeneous landscape adapt to local conditions in
71 the presence of migration, has a stronger bias towards alleles of large effect sizes (Griswold
72 2006, Yeaman & Whitlock 2011, Yeaman & Otto 2011). Third, interactions among genes
73 impacting phenotypes (*i.e.* epistasis) may alter the dynamics of adaptive variants, as
74 further discussed below.

75 In regards to the role of epistasis in adaptation, a discussion has existed since the
76 onset of the Modern Synthesis, with some arguing that it is largely irrelevant to the
77 trajectory of Darwinian selection (Fisher 1930, Cohan *et al*. 1989, Hill *et al*. 2008, Crow
78 2010) and others proposing that it plays an important role (Fenster *et al*. 1997, Hansen
79 2013, Wright 1931). The above literature suggests that on the one hand, epistasis might
80 not be expected to strongly affect adaptation because alleles at unlinked loci can segregate
81 independently and selection would act on the combined effect of each allele against
82 different genetic backgrounds; and yet, epistasis has the potential to alter the rate at which
83 adaptive trait changes can occur by producing larger or smaller effects in some of these
84 backgrounds, and in certain contexts, it may wield a stronger influence on the course of
85 adaptation.

86 Epistasis has been shown to play a role in many evolutionary processes, including
87 the evolution of sex and recombination, speciation, canalization, maintenance of genetic
88 variation, and the evolution of co-adapted gene complexes (Hansen 2013). How epistatic
89 interactions alter the response to directional selection is determined by the nature of the
90 epistatic interaction (Hansen 2013). Some kinds of epistasis affect the magnitude of the
91 phenotypic effects, such as positive and negative epistasis, and another kind, called sign
92 epistasis, changes the direction of the effect. Multiple theoretical and simulation studies

93 have investigated how each of these epistatic scenarios might influence the adaptive
94 process (Carter *et al.* 2005; Hansen *et al.* 2006; Yukilevich *et al.* 2008; Barton 2017). For
95 positive (synergistic) epistasis, in which the combined effect of both alleles is greater than
96 the sum of the individual effects, additive genetic variance would increase, and the mean
97 fitness in an adapting population is expected to change faster and reach a higher plateau
98 than without epistasis. For negative epistasis, in which the combined effect is lower than
99 the sum of the individual effects but still qualitatively consistent with the additive effects,
100 additive genetic variance decreases and the mean fitness during adaptation changes more
101 slowly and reaches a lower plateau than without epistasis. Particularly in the context of
102 adaptation, negative epistasis is also referred to as diminishing returns epistasis. For sign
103 epistasis, whether the allele will contribute to a larger or smaller phenotype will depend on
104 the allele at another locus. In this case, the evolutionary dynamics can be more complex,
105 and the fate of one allele is attached to the other, but while both variants persist, their
106 interaction may impede adaptation. Furthermore, to the extent that epistasis masks the
107 phenotypic influence of some variants, it may facilitate the accumulation of cryptic genetic
108 variation for a given trait, which may subsequently be exposed to selection when elements
109 of the genetic background (or the environment) change (Gibson & Dworkin 2004, Steiner
110 *et al*. 2007).

111 Despite the pervasiveness of epistasis at the genome-wide scale (Huang *et al*. 2012),
112 as well as between adaptive variants within proteins (Lunzer *et al*. 2010, Gong & Bloom
113 2014, Starr & Thorthon 2016), the prevalence of epistatic interactions among adaptive
114 variants that contribute to the evolution of more complex adaptive traits remains
115 incompletely understood. Studies of crop domestication have reported examples of

116 epistasis among artificially selected alleles, including grapevine varieties (Duchêne *et al*.
117 2012) and many examples in maize domestication (Stitzer & Ross-Ibarra 2018). Still,
118 compared to wild alleles, domesticated alleles were usually less sensitive to the genetic
119 background (reviewed in Doust *et al*. 2014). Epistasis was also found among adaptive
120 quantitative trait loci (QTLs) underlying flowering time in *Arabidopsis thaliana* (Juenger *et*
121 *al*. 2002). In a recent genome-wide screen in yeast, using genes known to be involved in a
122 high number of interactions, 24% of the adaptive variants were strain-specific and
123 indicative of epistasis (Ang *et al*. 2023). Positive epistasis has been shown to underlie the
124 evolution of bacteria with multiple antibiotic resistance alleles (Trindade *et al*. 2009).
125 Examples in animals involve epistasis between alleles underlying adaptive coloration in
126 butterflies (Papa *et al*. 2013), negative epistasis for traits underlying fitness in populations
127 of *Drosophila melanogaster* experimentally selected on a chronic larval malnutrition
128 regimen (Vijendravarma & Kawecki 2013), and epistasis between genes underlying coat
129 color in oldfield mice, in which the effect of one allele is only expressed in the presence of
130 another allele (Steiner *et al*. 2007).

131 The genetic architecture of adaptive traits can also be affected by gene-by-
132 environment interactions because the effect of a given allele can change depending on its
133 environment (Zeng *et al*. 1999, Mackay 2001). Examples of interactions between the
134 environment and adaptive alleles include *D. melanogaster* reproductive performance at
135 different temperatures (Fry *et al*. 1998), drought stress adaptation in wheat (Mathews *et al*.
136 2008), and local adaptation reflected in biomass for switchgrass (Lowry *et al*. 2019).
137 Similarly to epistatic interaction, gene-by-environment interaction can also uncover cryptic
138 genetic variation (Gibson & Dworkin 2004). The chaperone protein Hsp90 offers an

139 example of how genetic and environmental interactions can uncover cryptic variation
140 underlying discrete and continuous traits (Rutherford & Lindquist 1998, McGuigan & Sgro
141 2009, Flynn *et al.* 2020).

142 Here, we contribute to the understanding of the genetic architecture of adaptive
143 traits and the emerging knowledge about genetic and environmental interactions by
144 identifying adaptive quantitative trait loci (QTLs) underlying recent local adaptation in
145 natural populations of *D. melanogaster* and asking whether there is evidence of epistasis
146 among them and, for a subset, whether they interact with the environment. Using two
147 newly-described panels of recombinant inbred lines (RILs), we investigate several traits
148 that appear to have evolved directly or indirectly under adaptive differentiation between
149 an ancestral range population (Zambia) and a population from either France or highland
150 Ethiopia, regions colonized by *D. melanogaster* approximately 2 kya (Sprengelmeyer *et al.*
151 2020).

152 The traits examined here (cold tolerance, ethanol resistance, pigmentation, song
153 pattern, and wing length) show evidence of being either direct targets of local adaptation
154 or else pleiotropic readouts of local adaptation targeting correlated traits. The
155 pigmentation traits show strong correlations with environmental variables, especially
156 ultraviolet radiation (Bastide *et al.* 2014), which reaches particularly high levels in the
157 Ethiopian highlands. Larger wings may help Ethiopian flies navigate in cooler, thinner air,
158 and wing size was found to show unusually strong quantitative trait differentiation (Q_{ST} =
159 0.985; Lande 1992; Spitze 1993) between the Ethiopia and Zambia populations, compared
160 to genome-wide genetic differentiation (Lack *et al.* 2016), indicating a role for selection in
161 this trait's differentiation. France and Zambia have markedly different ethanol resistance,

162 also exceeding patterns of genome-wide genetic differentiation (Sprengelmeyer *et al.*
163 2021). Cold developmental survival shows a similarly consistent differentiation between
164 France and Zambia in particular (Huang *et al.* 2021), with clear presumptive adaptive value
165 in light of climate differences between these regions. A male song trait – the proportion of
166 pulses classified as slow (Clemens *et al.* 2018) – was included based on strong population
167 differentiation, with a Q_{ST} of 0.797 exceeding the F_{ST} of >96% of non-singleton SNPs (Lollar
168 *et al.* 2024). Although directional selection has not been previously reported to have acted
169 directly on song traits within *D. melanogaster*, it is also possible that this trait difference
170 reflects selection on a pleiotropically connected trait, such as synaptic function in a novel
171 thermal environment (Pool *et al.* 2017).

172 We also note that for the pigmentation, size, and ethanol resistance traits examined
173 here, bulk mapping studies found that all of these population trait changes had very
174 different genetic architectures from one mapping cross to the next (Bastide *et al.* 2016;
175 Sprengelmeyer *et al.* 2021; Sprengelmeyer *et al.* 2022). These results imply considerable
176 segregating variation in genetic basis of each trait difference within one or both of the
177 populations studied. However, it is possible (though as yet untested) that epistasis may
178 also play a role in yielding distinct QTLs in different mapping crosses for these traits.

179 For each of the above traits, we first identify QTLs and candidate genes that may
180 underlie each of these traits. Then, we quantify the strength of evidence for epistasis
181 impacting each detected QTL, and then assess the overall signal of epistasis across traits.
182 Lastly, we investigate the reaction norm of the QTLs underlying a subset of the traits,
183 related to pigmentation, that were studied in two different temperature treatments. These

184 investigations provide new insights into both the genetic basis of adaptive trait changes
185 and the dependence of adaptive alleles on genetic interactions.
186
187 **Methods**

188 ***Mapping cross design***

189 We report two new Recombinant Inbred Line (RIL) mapping panels of *Drosophila*
190 *melanogaster*. Each RIL set was derived from a cross between two inbred lines from
191 distinct geographic populations, in each case pairing a strain from the southern-central
192 African ancestral range of the species (Sprengelmeyer *et al*. 2020) with a strain from a
193 cooler derived environment. One cross was between a Zambian inbred line (ZI215N,
194 BioProject PRJNA861300) and a highland Ethiopian inbred line (EF43N, sequenced in Lack
195 *et al*. 2016); the other was between a different Zambian inbred line (ZI418N, sequenced in
196 Sprengelmeyer & Pool 2021) and a French inbred line (FR320N, sequenced in Lack *et al*.
197 2016). Each cross was allowed to interbreed in an intercross design for 13 and 12 non-
198 overlapping generations, in the Ethiopian and French cross, respectively. Then, the
199 offspring of individual females were inbred for 5 generations to create each RIL. We
200 obtained 293 and 328 RILs for the Ethiopian and French panels, respectively (BioProject
201 PRJNA861300). The Zambian lines were collected in Siavonga, the Ethiopian line was
202 collected in Fiche, and the French line was collected in Lyon (Lack *et al*. 2015).
203
204 ***Phenotypes***

205 Ethiopian flies have increased wing area, even after correcting size relative to their
206 larger body mass (Lack *et al*. 2016). We measured the wing length of female flies that were
207 at least 3-days old. 10 female flies per RIL were photographed using an Amscope SM-4TZZ-

208 144A dissection microscope under CO_2 anesthesia. The pictures were scored with ImageJ
209 (Abramoff *et al*. 2004). Wing length was measured as the distance from the intersection of
210 the L4 longitudinal vein and the anterior cross vein to the L3 longitudinal vein intersection
211 with the wing margin.

212 Ethiopian flies are darker than Zambian flies (Bastide *et al*. 2014). We
213 photographed and measured two to five females per RIL using a dissection scope.
214 Resolution (3584 x 2748 pixels), gain (3.0), exposure time (99.84 ms), magnification (20x),
215 and illumination level were kept constant using an Amscope adaptor for LED lamp at
216 maximum lighting. White balance was set at the same resolution using ColorChecker white
217 balance. We measured three common traits for pigmentation: the pigmentation of the
218 mesopleuron in greyscale proportion ranging from 0 for white to 1 for black (herein,
219 mesopleuron, a thorax trait), the pigmentation of the background of the fourth abdominal
220 segment in the same greyscale proportion (herein, A4 Background), and the proportion of
221 the fourth abdominal segment that was covered by the black stripe (herein, stripe ratio).
222 Relatively low correlations among these three traits were observed among independent
223 isofemale strains within the Ethiopia and Zambia populations ($r < 0.35$), except for a
224 higher correlation between mesopleural and A4 Background for Ethiopia specifically ($r =$
225 0.646; Bastide *et al*. 2014).

226 Pigmentation is also plastically influenced by temperature, and the Ethiopian
227 population is located in a colder region, on a high plateau 3 km above sea level. Therefore,
228 we measured the three pigmentation traits in flies raised at two temperatures (25 °C and
229 15 °C), to uncover potential cryptic variation that could be present in the warmer Zambian
230 (midpoint temperature: 25 °C) but is only expressed in the colder Ethiopian (midpoint

231 temperature: 11 °C) population. We also report plasticity for these three pigmentation
232 traits, as the difference in the trait measured at 25 °C and 15 °C.

233 French flies have higher resistance to ethanol (Cohan & Graf 1985, Sprengelmeyer &
234 Pool 2021) and cold (Pool *et al*. 2017, Huang *et al*. 2021) than Zambian flies. Ethanol
235 resistance was measured as the average time 300 female flies, 3- to 5-day old, from each
236 RIL needed to become immobile when exposed to 18% ethanol. The flies were placed in 50
237 ml falcon tubes with ethanol-saturated tissue placed on the bottom, and the number of
238 mobile flies was scored every 15 minutes for six hours. Cold tolerance was measured as
239 egg to adult survival when raised at 15 °C (Huang *et al*. 2021).

240 The song pattern trait was the ratio of slow pulses over all pulses (slow and fast) in
241 the song made by males during courtship. Although not expected to be under local
242 environmental selection *a priori*, male courtship is often under strong sexual selection. In
243 addition, a large number of nervous system genes appear to have evolved between warm-
244 and cold-adapted *D. melanogaster* populations (Pool *et al*. 2017), representing one
245 potential source of pleiotropic effects on song traits. We found that Zambian male flies
246 display a greater fraction of slow to fast pulses than French flies, a novel pulse mode
247 classification recently discovered within the *D. melanogaster* species complex (Clemens *et*
248 *al*. 2018). The song data was recorded in the Stern Lab at Janelia Farms Research Campus,
249 using materials and methods described by Arthur and colleagues (Arthur *et al*. 2013). Song
250 was annotated without human intervention with SongExplorer (Arthur *et al*. 2021).
251 Annotations were classified with locally modified versions of BatchSongAnalysis
252 (https://github.com/dstern/BatchSongAnalysis), using previously trained *D. melanogaster*
253 models provided by Ben Arthur (Lollar *et al*. 2024).

254 We expected that there might be some level of correlation among the traits of any
255 given cross purely due to either linkage among causative variants or else pleiotropy. We
256 calculated the pairwise correlation between all the traits measured for each cross to
257 investigate the degree to which they are correlated.
258
259 ***DNA Extraction and Sequencing***
260 For each RIL, we extracted DNA from five to ten female flies from each line. The flies
261 were crushed and homogenized using pipette tips in strip tubes, in a solution of 100 µl of
262 lysis buffer (50 mM Tris-HCl with pH = 8, 100 mM EDTA, 100 mM NaCl, and 0.5% SDS)
263 and 2 µl of proteinase K (IBI Scientific). The samples were incubated to inactivate the
264 proteinase K (55 °C for 5 minutes, 95 °C for 10 minutes, and 25 °C hold). The supernatant
265 of the fly lysate was transferred to new tubes, and we added SPRI beads (Sera-mag
266 SpeedBeads SPRI beads, [GE Healthcare 24152105050250]) in a 1.8 to 1 proportion of
267 beads to lysate. The beads were used in a solution of PEG 8000 (9 g), Tween 20 (27.5 µl),
268 5M NaCl, and 3 mL TE Buffer (composed of 100 µl of 1 mM EDTA, 500 µL of 10 mM Tris
269 HCl). 1 mL of the beads were added to the buffer mix and filled with water until the final
270 volume was mL. The tubes were incubated for at least three minutes at room temperature
271 for DNA to bind to the beads and then placed on a magnetic plate for five minutes to
272 remove the beads from the solution. The supernatant was discarded, and the beads were
273 washed with two rounds of 80% ethanol (90 µL per well). DNA was eluted beads with 30
274 µL of H_2O and then used the magnetic plate to transfer only the resuspended DNA to new
275 tubes.
276 Genomic libraries were prepared following Adams *et al.* (2020), with size selection,
277 cutoff at 300 bp, and cleanup performed using the Zymo Select-a-Size DNA clean &

278 Concentrator [catalog No. D4080]. Libraries were sequenced at the UW-Madison
279 Biotechnology Center on the Illumina NovaSeq 6000 platform, with 150bp pair-ended
280 reads.
281
282 ***DNA Alignment and Ancestry Calling***

283 The reads were mapped to the *D. melanogaster* (v5.57) reference genome using
284 BWA-MEM, version 0.7.17 (Li 2013). We used Ancestry HMM (Corbett-Detig & Nielsen
285 2017) to estimate ancestry along the genome of each RIL, allowing for diploid ancestry
286 calls (*i.e.* homozygous for either parent, or heterozygous). Ancestries were summarized in
287 windows defined to contain 1,000 SNPs in the Zambian population (~19kb average size),
288 using the majority ancestry call in the case of an ancestry breakpoint within the window.
289 We used a recombination map based on Comeron *et al.* (2012) but modeled only one
290 generation of recombination when using Ancestry HMM, in order to focus on
291 conservatively-defined ancestry switches (pipeline available on
292 https://github.com/ribeirots/RILepi).
293
294 ***QTL Mapping***

295 To test whether adaptive loci showed evidence of epistatic interactions we first used
296 QTL mapping to identify the adaptive loci and then performed epistasis tests between the
297 focal loci and all other loci in the genome. Each locus is a genomic window of ~19kb,
298 defined and genotyped as described above.

299 To identify loci underlying trait changes, we reimplemented the R/qtl (Broman *et al.*
300 2003) *scanone()* function in an additive framework using Python3 (Van Rossum & Drake
301 2009), modifying the genotypes to be coded as numeric variables instead of categorical

302 (https://github.com/ribeirots/RILepi). This modification was preferred in light of the
303 small counts of specific genotypes due to low heterozygosity and genomic ancestry skew
304 present in our RIL panels.

305 The initial QTL mapping is based on the comparison of a model with a single QTL
306 *versus* a model without any QTL, performed repeatedly one locus at a time. For each locus,
307 we obtained a logarithm of the odds (LOD) score as the ratio between the log-likelihoods of
308 the model with one QTL over the model without a QTL. Because both RIL sets had average
309 ancestral frequencies skewed against the Zambian ancestry (68% Ethiopia ancestry and
310 75% France ancestry), we excluded the windows with an ancestry bias of 90% or greater
311 for either ancestry to avoid the effects of extremely uneven sample sizes on the model. The
312 genome-wide significance of a QTL was tested using 10,000 permutations, in which trait
313 values were randomly shuffled. From each permutation, we saved the highest LOD score
314 obtained for any window (excluding windows with ancestry skew of 90% or greater) and
315 empirical LOD scores from each window were compared to the null, permutation LOD
316 score distribution. We considered the windows whose LOD score's p-value was lower than
317 0.10 as putative QTLs (*i.e.* a less than 10% chance of having a QTL signal of that strength
318 anywhere in the genome). A p-value threshold of 0.10 was chosen aiming to include a
319 sufficient number of QTLs to be tested for epistasis. Each putative QTL surrounded by
320 windows with a lower LOD score was considered a putative QTL peak. If two putative QTL
321 peaks were not separated by a window with a LOD score lower than the minor peak's LOD
322 score minus 1.5, the minor peak was removed. Finally, the remaining putative QTL peaks
323 were filtered to remove any peak within 10 cM of a QTL peak with a higher LOD score, in
324 order to increase the independence of QTLs used in epistasis testing. The confidence

interval for these QTLs was defined as all contiguous windows with a LOD higher than the QTL's peak LOD score minus 1.5.

Candidate Genes and Population Genetics

To identify genes potentially underlying the adaptive traits, we scanned our QTL regions for signatures of local adaptation based on populations genetics. We used sequenced genomes from inbred lines from each of the studied populations to calculate a haplotype-based statistics: χ_{MD} (Lange & Pool 2016) and two F_{ST} statistics (using Reynolds *et al*. 1983), $F_{ST_FullWin}$ (window-wide F_{ST} calculated using all the SNPs in the window) and F_{ST_MaxSNP} (the highest F_{ST} value from a single SNP within the window), that have power to distinct power to detect distinct kinds of selective events (da Silva Ribeiro *et al*. 2022). We defined as outlier windows those that fell within the top 1% of windows on the same chromosome arm for any of the above three statistics. We focused on regions with recombination rates generally above 0.5 cM/Mb (Comeron *et al*. 2012) due to more localized signatures of selection: 2.3–21.4 Mb of the chromosome X, 0.5–17.5 Mb of arm 2L, 5.2–20.8 Mb of arm 2R, 0.6–17.7 Mb of arm 3L, and 6.9–26.6 Mb of arm 3R. We selected as candidates all genes that overlapped with the outlier windows as well as the first gene up- and down-stream of the outlier window, to account for instances in which the target of selection is in a regulatory region outside the gene region. We also identified other genes within these QTLs with a known or potential association with the phenotype.

Epistasis Testing

Epistasis tests were performed between each focal QTL and all of the remaining genomic windows outside its confidence interval. The epistasis test for each window pair

349 consisted of an interaction LOD score obtained as the ratio between the log-likelihoods of
350 the model with two QTLs and their interaction (y ~ Q1 + Q2 + Q1:Q2) *versus* a model
351 including both QTLs but no interaction (y ~ Q1 + Q2). The interaction LOD score for each
352 pair was compared against permutations. Permutations were specific for each QTL
353 analyzed. We shuffled the phenotype, fixed the focal QTL (Q1), and calculated the
354 interaction LOD score of Q1 against all other windows in the genome. The highest
355 genomewide interaction LOD score from each permutation was kept and the empirical
356 interaction LOD scores were compared against this null, permuted interaction LOD
357 distribution.
358
359 ***Epistasis Meta-analysis***
360 We combined the results from all the epistasis tests across mapping crosses and
361 phenotypes to test the hypothesis of whether adaptive QTLs have epistatic interactions.
362 We collected the set of epistasis p-values from each QTL and its most likely interactor,
363 which quantify the probability of obtaining any interaction term between that QTL and any
364 partner locus in the genome with an interaction LOD score as high as the one observed. We
365 used Fisher's combined probability test to ask if the p-values from each QTL and their most
366 likely interacting locus reject the null hypothesis that there is no epistasis. The p-values
367 should follow a uniform distribution if the null hypothesis is true. Therefore, we performed
368 an additional step to investigate how many of the lowest p-values would need to be
369 removed from the data set to obtain a median value near 0.50, in order to ask whether our
370 cumulative data set showed any hints of epistasis across all analyzed QTLs.
371
372 ***Epistasis Power Analysis***

373 We calculated the power of our approach and our data sets to detect an interaction
374 by simulating phenotypes with different interaction strengths. We chose one empirical
375 QTL with intermediate sample size and estimated the additive QTL effect among the
376 detected QTL to serve as the basis for the simulations. The QTL chosen was detected for
377 the abdominal background pigmentation at 25 °C, it had an estimated effect size equal to
378 0.035, mean trait value equal to 0.3485, and a standard deviation equal to 0.0697. The
379 observed genotype distribution of the QTL peak window was used for the simulations. Our
380 null simulations generated phenotypes based on a normal distribution with the observed
381 trait mean and standard deviation, and the simulated values were modified based on the
382 trait effect and individual genotypes (1x effect for heterozygous and 2x effect for non-
383 Zambian homozygous). We then calculated the interaction LOD score of the focal peak
384 window against all other genome windows outside the original QTL's confidence interval
385 and kept the highest genomewide interaction LOD score obtained. We repeated this
386 process 10,000 times to obtain a null (no interaction) distribution of interaction LOD
387 scores.
388 To simulate epistasis, we used the genotype distribution of the window most likely
389 to be interacting with our focal QTL: the window with the highest empirical interaction
390 LOD score. We modified the effect of the focal QTL on the simulated phenotype based on
391 the genotype of the interacting window. If the genotype of the interacting window was
392 Zambia homozygous, the original effect was not modified, if it was non-Zambian
393 homozygous, the original effect was multiplied by the interacting factor I, and if the
394 genotype of the interacting window was heterozygous, the original effect was intermediate,
395 (i.e. multiplied by $(1+I)/2$). We simulated positive epistasis effects (original effect

396 increased by the presence of the epistatic allele) ranging from 1.125 to 4. For diminishing
397 returns negative epistasis, we simulated negative epistasis effects (original effect
398 decreased by the presence of the epistatic allele) from 0.889 (1/1.125) to 0.5. For sign
399 epistasis (the original effect changes in sign, e.g. instead of producing larger trait it
400 produces smaller traits), we examined effects from -0.5 to -2. We also simulated masking
401 epistasis (the original effect is nullified in the presence of the epistastic allele) with effect I
402 $= 0$.

403 Each interaction simulation was compared against the null distribution and a p-
404 value was calculated as the proportion of null simulations with an interaction LOD score
405 higher than the simulated interacting LOD score. Power was calculated for each interaction
406 effect I as the proportion of simulations that had p-value lower than 0.05.

407 We also calculated the power of our meta analysis based on 13 QTLs' interaction p-
408 values. For each interaction effect, we sampled 13 interaction LOD score p-values and
409 calculated (1) how often the fisher combined p-value was as extreme or greater than the
410 one we observed and (2) how often at least one p-value was lower than the lowest p-value
411 we obtained for our empirical data.

412

413 ***Reaction Norms***

414 To investigate genotype-by-environment interactions for pigmentation traits, we
415 combined phenotypic data from RILs raised at the two temperature treatments (15 °C and
416 25 °C) with the genotype of each non-overlapping QTL. To test whether the genotype-by-
417 environment interaction was significant, we used a linear model with the phenotype as the

418 response variable and the genotype, environment, and genotype-by-environment

419 interaction as the explanatory variables.

420
421
422
423 **Results**

424 ***Genotype and phenotype data***

425 Whole genome sequences for the RILs had mean depth of coverage of 3.3X (S.D.

426 1.96, Table S1) and 7.58X (S.D. 9.09, Table S2) per site for EF and FR RILs, respectively,

427 which should be more than sufficient to call population ancestry in large chromosomal

428 blocks. Ancestries for both RIL sets were skewed toward lower Zambian ancestry, with

429 averages of 67.84% Ethiopian ancestry and 77.88% French ancestry. After five generations

430 of inbreeding, a low level of parental strain heterozygosity was present in the final panel:

431 8.71% and 5.3% on the Ethiopian and French panels, respectively (at the level of genomic

432 windows). The sample size varied for each trait based on the number of RILs successfully

433 phenotyped (Table 1, S1, S2).

434

435 **Table 1.** Summary of mapped traits. Listing the mapping cross used for each trait (EF =

436 Ethiopia, FR = France), the number of phenotyped lines for each trait, the number of QTLs,

437 and the number of QTLs with epistatic interaction for each phenotypic trait.

RIL panel	Trait	Sample size	# QTLs
EF	A4 Background 25 °C	278	1
EF	Stripe Ratio 25 °C	278	1
EF	Mesopleuron 25 °C	278	1
EF	A4 Background 15 °C	190	0
EF	Stripe Ratio 15 °C	190	1

EF	Mesopleuron 15 °C	190	1
EF	A4 Background (Plast.)	178	0
EF	Stripe Ratio (Plast.)	178	0
EF	Mesopleuron (Plast.)	178	0
EF	Wing Length	268	5
FR	Cold Tolerance	304	0
FR	Ethanol Resistance	277	3
FR	Song Pattern	294	1

438

439 Correlations among the analyzed traits were examined for each RIL panel, which
440 may indicate pleiotropy or else linkage of causative alleles. Among pigmentation traits, the
441 thoracic mesopleuron trait was strongly correlated with abdominal background (Table
442 S3). Stripe width showed moderate, significant correlations with both of those traits at 25
443 °C but weaker correlations at 15 °C. Abdominal background showed a non-significant
444 correlation between the two temperatures, while the other two traits showed moderate,
445 significant correlations between temperatures. In light of the correlations observed among
446 many pigmentation traits, overlapping QTLs for pigmentation traits were not treated as
447 independent QTLs, and only the QTL with the highest LOD score was used in downstream
448 analyses. No pigmentation trait was significantly correlated with wing length (Table S3),
449 the only other trait scored among the Ethiopian RIL panel. Among traits scored from the
450 French RIL panel, the song pattern was weakly correlated with ethanol resistance, $r^2 = 0.13$
451 (Table S4).

452

453 ***Single locus QTL mapping***

454 We identified potential QTLs for eight out of the thirteen investigated traits (Figure
455 1; Table 1). The traits with no detected QTLs were A4 Background at 25C, all the three

456 pigmentation plasticity traits, and cold tolerance. The number of QTLs per trait ranged up
457 to five, for wing length, with other traits yielding one or three QTLs (Figure 1, Table 1).
458 Twelve of the fourteen QTLs were significant at $p < 0.05$, while two marginally significant
459 QTLs - one for A4 Background at 25 °C ($p = 0.0591$) and one QTL for ethanol resistance (p
460 $= 0.0693$) – were also considered in downstream analyses (Table 2).

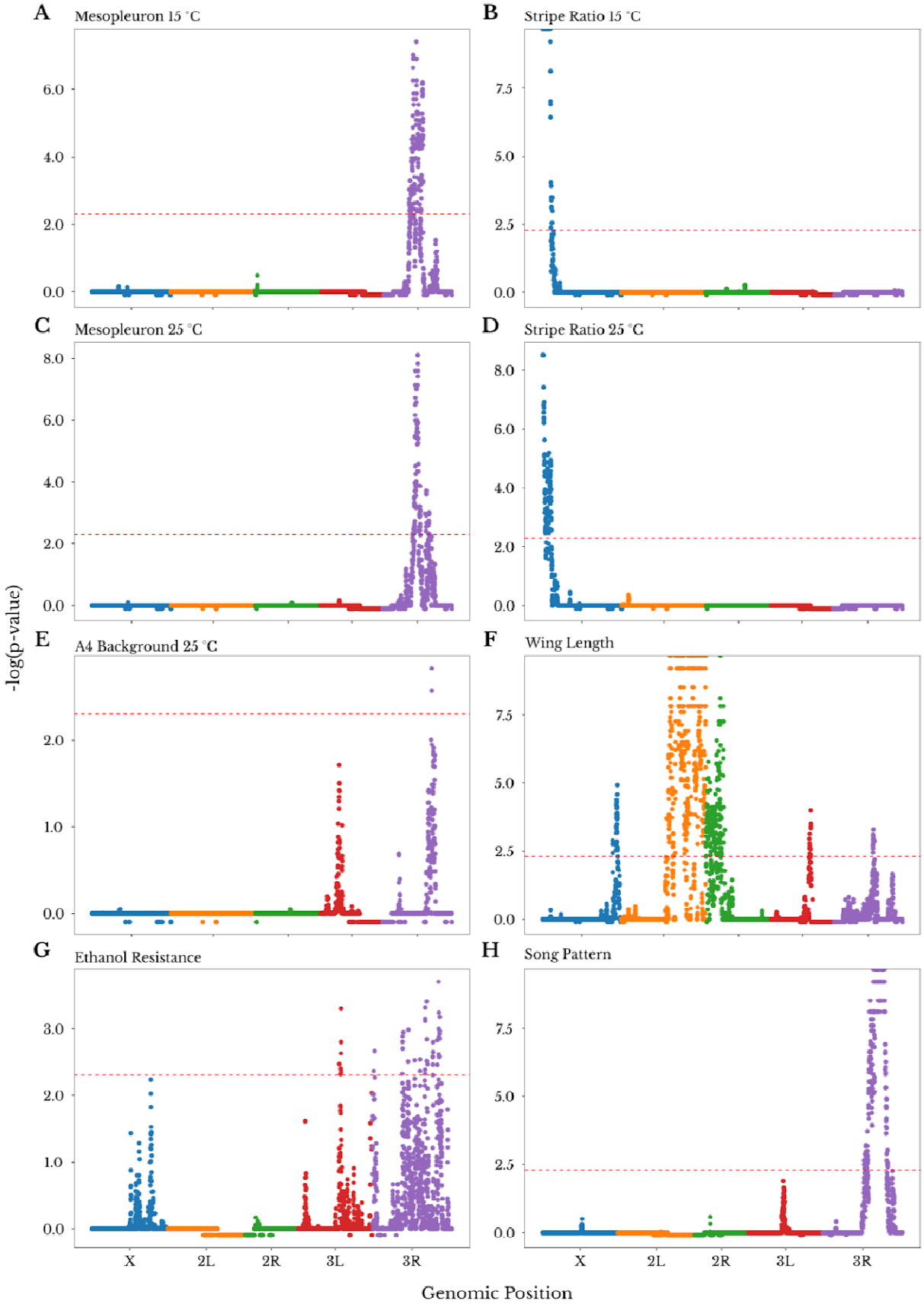
A
Mesopleuron 15 °C
B
Stripe Ratio 15 °C
C
Mesopleuron 25 °C
D
Stripe Ratio 25 °C
E
A4 Background 25 °C
F
Wing Length
G
Ethanol Resistance
H
Song Pattern
-log(p-value)
X
2L
2R
3L
3R
Genomic Position

461

462 **Figure 1.** The number of QTLs for each trait ranged from 0 to 5. In this figure, only the traits
463 with at least one identified QTL are shown; the traits without QTLs (Table 1) can be seen in
464 Figure S1. Each panel shows the -log of the p-value for the LOD score of the genomic
465 windows. A4 Background (Figure 1E) is shown here with no QTL above the threshold, but
466 one marginally significant QTL (p-value = 0.053, Table 2). Windows filtered out for
467 ancestry skew are given a value of -0.25. The red dashed line represents the 0.05 p-value
468 cutoff based on 10,000 permutations. The color of the dots represents the chromosome
469 arm of each genomic window. Note that for wing length, a single QTL spans a broad low
470 recombination centromeric region between 2L and 2R.
471
472 **Table 2.** Characteristics of detected QTLs for all analyzed phenotypes. The single QTL
473 coefficient shows the magnitude of phenotypic change by substituting one allele of the
474 derived population ancestry at that locus, which is shown on the scale of the measured
475 phenotype. The correlation coefficient r^2 shows how well QTL genotype predicts
476 phenotypic variation (how well the data fits the model). QTL p-value and epistasis p-value
477 were obtained based on 10,000 permutations. * an estimated p-value of zero means the
478 empirical value was more extreme than any permutation. A LOD score and CI in italics
479 indicate a QTL that was excluded from subsequent meta-analysis due to a stronger
480 overlapping QTL for a correlated trait. Further details of each QTL are given in Table S5.

RIL panel	Trait	LOD score	Trait Coeff.	r^2	QTL p-value	QTL Confidence Interval	Epist. p-value
EF	A4Back 25C	3.274	0.012	0.053	0.0591	Chr3R:21,614,478..22,512,754	0.736
EF	Mesopl 15C	5.819	0.012	0.132	0.0006	Chr3R:16,750,589..16,945,416	0.699
EF	Mesopl	5.890	0.014	0.093	0.0003	Chr3R:17,549,430..17,666,763	0.714

	25C						
EF	Stripe 25C	*6.335*	0.035	0.100	0.0002	*ChrX:0..2,141,596*	0.643
EF	Stripe 15C	9.924	0.071	0.214	0*	ChrX:1,057,169.. 2,420,139	0.244
EF	Wing	9.581	0.026	0.153	0*	Chr2L:12,902,781..13,046,286	0.322
EF	Wing	8.628	0.024	0.139	0*	Chr2L:22,740,849..23,011,543	0.672
EF	Wing	3.867	0.022	0.065	0.0183	Chr3L:10,353,468..11,407,946	0.444
EF	Wing	3.526	0.019	0.059	0.0369	Chr3R:18,722,896..19,232,530	0.941
EF	Wing	4.286	0.016	0.072	0.0073	ChrX:20,419,847.. 20,893,609	0.183
FR	EtOH	3.565	22.516	0.059	0.0368	Chr3L:10,829,907..11,166,414	0.208
FR	EtOH	3.253	27.506	0.054	0.0693	Chr3R:3,268,049..3,791,969	0.853
FR	EtOH	3.740	19.166	0.061	0.0246	Chr3R:23,770,233..24,580,087	0.476
FR	Song	9.111	0.019	0.133	0*	Chr3R:21,997,113..22,171,358	0.273

Of the five pigmentation QTLs, the two identified for stripe ratio (one at 25 °C and one at 15 °C) overlapped, and only the one with the highest LOD score (15 °C) was retained for meta-analysis (Table S5). Confidence intervals for the two QTLs detected for mesopleuron (one at 25 °C and one at 15 °C) were separated by just over 600 kb, so they were kept as two independent QTLs for the meta-analysis (Table 2).

The effect of all QTLs (Table 2) was in the expected direction: substituting alleles of the derived population resulted in phenotypic changes in the direction of the derived populations. This pattern is congruent with a scenario where these QTLs are contributing to locally adaptive trait changes (involving either the measured traits or else pleiotropically correlated traits under selection), given that if the phenotypic difference were neutral, we would expect some QTLs to show an effect in the opposite direction (Orr 1998).

494 ***Outlier and Candidate Genes within QTLs***

495 To generate hypotheses for possible causative genes underlying trait changes, we
496 used population genetic summary statistics to identify genes within our QTLs that are
497 potentially under local adaptation. Specifically, we flagged genes associated with windows
498 that fell within the chromosome arm's top 1% of windows for window F_{ST}, maximum SNP
499 F_{ST}, or the haplotype statistic χ_{MD} (Table 3). These local adaptation scans were not
500 conducted in low recombination QTL regions due to the expected lack of gene-scale
501 resolution of selection signals in such genomic intervals. Since a striking signal of local
502 adaptation is not guaranteed at loci underlying these strong population trait differences,
503 we also noted the presence of other functionally relevant candidate genes within each QTL.
504

505 **Table 3.** QTL traits, confidence interval, and candidate genes detected by a priori functional
506 knowledge or as population genetics outliers (n/a indicates that QTL was in a region of low
507 recombination and was not analyzed for signatures of selection).

Trait	QTL Confidence Interval	Candidate Genes	Genes with Signatures of Selection
A4Back 25C	Chr3R:21,614,478.. 225,12,754		*TwdlQ, beat-vii, scrib*
Meso 15C	Chr3R:16,750,589.. 16,945,416		
Meso 25C	Chr3R:17,549,430.. 17,666,763	*burs*	
Strp 25C	ChrX:0..2,141,596	*Hr4, y*	n/a
Strp 15C	ChrX:1,057,169.. 2,420,139	*Hr4*	n/a
Wing	Chr2L:12,902,781.. 13,046,286		*A16, Vha68-2, ACXE, CG16800, Tor, Ube4B*
Wing	Chr2L:22,740,849..	*Slmap*	n/a

	23,011,543		
Wing	Chr3L:10,353,468.. 11,407,946	*Cpr67Fa2, FoxK, Rbfox1, scyl, wls*	*Fad2, CG32079, klu*
Wing	Chr3R:18,722,896.. 19,232,530	*Cow, Gbp3, hh, lrk1, p53, pnt, Rassf*	*Pnt*
Wing	ChrX:20,419,847.. 20,893,609		*CG15450, Cyp6v1, hydra, shakB, CG1835, CG11227*
EtOH	Chr3L:10,829,907.. 11,166,414	*Aps*	*CG42831, tna*
EtOH	Chr3R:3,268,049.. 3,791,969		n/a
EtOH	Chr3R:23,770,233..24,580,087	*fkh*	*trv, htt, CG34354, CG43125, snu*
Song	Chr3R:21,997,113.. 22,171,358		

The mesopleuron pigmentation QTL detected at 25 °C included the gene *burs* (Dewey *et al*. 2004), implicated in cuticle tanning and hardening. The two stripe ratio QTLs, at the beginning of chromosome X, both included the candidate gene *Hr4*, a gene that when suppressed results in reduced pigmentation (Rogers *et al*. 2014). One also included the gene *yellow*, canonically implied in pigmentation variation and evolution (e.g. Massey & Wittkopp 2015). This pair of QTLs overlapped others previously detected for the same trait in distinct Ethiopia-Zambia crosses (Bastide *et al*. 2016). The gene *ebony*, at which a soft sweep signal associated with a pigmentation QTL was previously characterized for Ethiopian *D. melanogaster* (Bastide *et al*. 2016), fell just between the closely-located Meso15C and Meso25C peaks.

At least one gene related to wing development was found within each of the five wing length QTL regions. Within the distal 2L QTL, our population genetic outliers included the *Drosophila* target of rapamycin gene (*Tor*), which plays a key role in insulin

523 signaling and growth regulation, and has been tied to wing size and development
524 specifically (Parker & Struhl 2015). Outliers inside this QTL also included the potential
525 wing regulators *Vha68-2* and *Ube4B* (Krupp *et al*. 2005, Blanco *et al*. 2010, Okada *et al*.
526 2016, López-Varea *et al*. 2021). Within the low recombination distal 2L wing QTL, among
527 the few genes present was *Slmap*, a hippo signaling gene shown to alter wing size (Zheng *et*
528 *al*. 2017). Within the 3L wing QTL, population genetic outliers included *klu*, which
529 regulates cell size and proliferation, and is associated with wing size defects (Schertel *et al*.
530 2015). Within the 3R QTL, outliers included *pnt*, related to wing morphogenesis (Dworkin
531 & Gibson, 2006, Bejarano *et al*. 2008, Paul *et al*. 2013). The X-linked wing QTL on
532 chromosome X included an outlier gene possibly involved in wing development, *shakB*
533 (Krishnan *et al*. 1993). Three of those QTLs (X, 2L proximal, and 3L) overlap with
534 previously detected wing length QTLs, each from a different Ethiopia-Zambia cross out of
535 four previously analyzed mapping crosses (Sprengelmeyer *et al*. 2020).
536 For the ethanol resistance QTLs, we identified two population genetic outlier genes
537 (*htt* and *trv*) previously implicated in response to ethanol within the distal QTL on
538 chromosome 3R (Fochler *et al*. 2017). Outlier genes detected within the other two QTLs
539 had no annotated connection to ethanol. These QTLs did not overlap with those previously
540 detected for the same trait from distinct France-Zambia crosses (Sprengelmeyer *et al*.
541 2021), in line with the genetically variable basis of this trait identified by that study.
542 Overall, we identified both novel genes underlying the studied traits and genes that
543 had already been implicated with their respective trait. The identification of genes already
544 known to underlie these traits (although in many cases not their evolution) provides
545 support for the approach we used here.

546
547 *Epistasis*

548 To investigate whether there is evidence of epistasis among adaptive loci, we
549 performed an epistasis scan for each single QTL and a meta-analysis combining the results
550 across non-correlated traits. We did not identify any individually significant epistatic QTL
551 pairs. The lowest genome-wide interaction LOD score p-value we obtained was 0.183, for a
552 wing length QTL (Table 2).

553 Our meta-analysis of the combined non-overlapping single QTLs also supports the
554 hypothesis that there is no strong epistasis involving adaptive loci. By combining the
555 interaction p-values for all non-overlapping QTLs (where each p-value denotes the
556 probability of that QTL having any interaction LOD effect that strong in the genome, based
557 on 10,000 permutations), we obtained a p-value of 0.763 using Fisher's combined
558 probability test. This result indicated that the observed p-values do not deviate from the
559 null expectation of uniformly distributed p-values expected without epistasis involving
560 adaptive loci.

561 Because our sample sizes of RILs may not be suitable for detecting all magnitudes of
562 epistasis, we conducted a simulation-driven analysis to indicate the strength of our
563 negative results, and to indicate if there was a parameter space of epistasis that we could
564 confidently rule out based on these results. Based on this analysis, our method had a high
565 power (over 80%) to detect an epistatic QTL pair in scenarios of sign epistasis, in which the
566 interaction effect changed the direction of the main effect, as well as high power to detect
567 strong positive epistasis in which the interaction effected increased the main effect at least
568 2.5-fold (Figure 2, Table S6). We also tested the power of our meta-analysis by re-sampling
569 13 p-values from simulated data sets of different interaction effects (Figure 2). This

570 analysis indicated that we should have had power to detect similar scenarios of strong
571 epistasis as indicated for the lowest p-value analysis above (*i.e.* sign epistasis and positive
572 epistasis at least doubling the main effect, and that we would likely have detected masking
573 epistasis as well, in which the main effect was erased by the modifier). Therefore, the lack
574 of detected epistatic interactions from our empirical data supports the hypothesis that such
575 strong forms of epistasis did not play an important role in these instances of evolution.

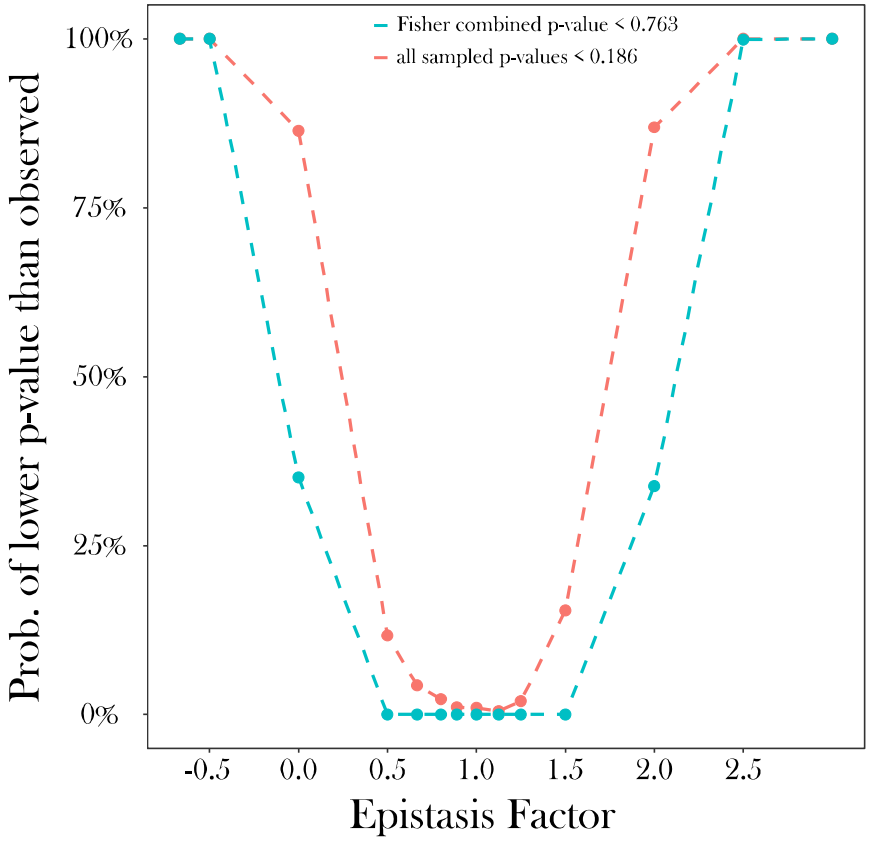

576

577 **Figure 2.** Simulation analysis indicating that strong positive epistasis or sign epistasis
578 should have been detectable for the empirical data. Simulations based on randomly
579 permuted individual genotypes and simulated epistatic effects (see Materials and Methods)
580 were conducted to assess our ability to detect varying models of epistasis based on either
581 the lowest empirical epistasis p-value (red series) or the Fisher-combined epistasis p-value

582 across 13 analyzed QTLs (blue series). Here, the epistasis factor (x-axis) represents the
583 multiplier that a modifier locus exerts on the primary QTL's effect. Thus, negative values
584 represent sign epistasis, zero represents masking epistasis, values less than 1 indicate
585 negative epistasis, and values above 1 indicate positive epistasis. The y-axis shows the
586 proportion of occurrences out of the 1,000 resampled instances in which a given model of
587 epistasis yielded a lowest p-value lower than the observed 0.183 (red), or else how often
588 the combined Fisher p-value was lower than the observed 0.763 (blue).
589

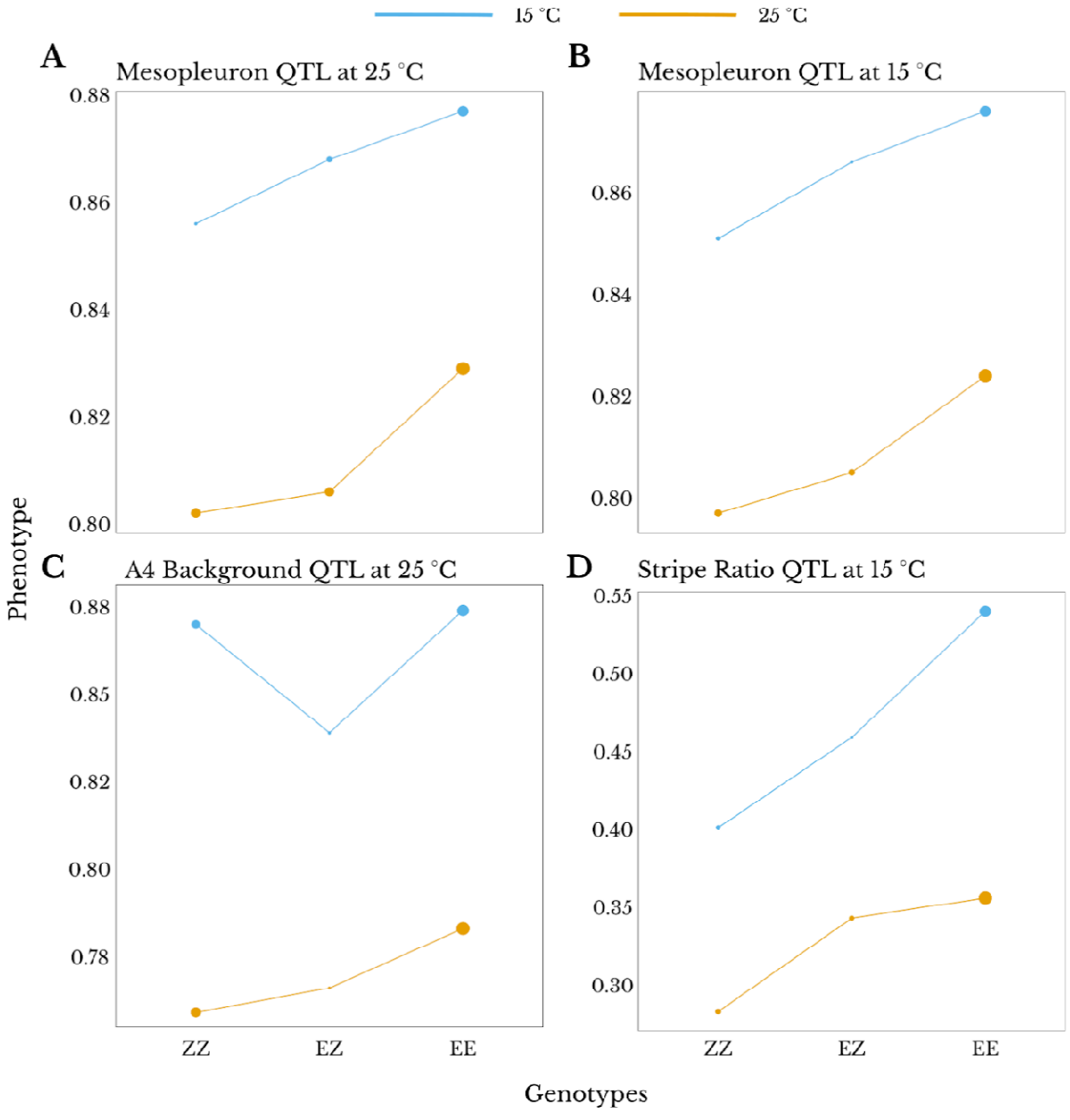

Figure 3. The reaction norms of the four non-overlapping pigmentation QTL show darker phenotypes for flies raised at 15 °C than at 25 °C and for flies with Ethiopia ancestry alleles, corroborating expectations. (A) Mesopleuron at 25 °C, QTL on chromosome 3 with peak position from 17,566,218 to 17,600,070. (B) Mesopleuron at 15 °C, QTL on chromosome 3R with peak position from 16,773,298 to 16,788,420. (C) A4 Background at 25C, QTL on

596 chromosome 3R with peak from 21,614,478 to 21,628,049. (D) Stripe ratio at 15 °C, QTL
597 on chromosome X with peak from 1,246,761 to 1,303,582. The y-axis shows the mean
598 phenotype for each genotype and temperature treatment; a higher number is a darker
599 phenotype. ZZ = Zambia homozygous, EZ = heterozygous, EE = Ethiopia homozygous.
600

601 ***Phenotype plasticity for pigmentation QTLs***

602 Fly pigmentation is known for its temperature-based plasticity; flies reared at lower
603 temperatures develop darker phenotypes than those raised at warm temperatures (David
604 *et al.* 1990). Our results recapitulated this behavior, in that average pigmentation traits
605 were higher (*i.e.* darker) at 15 °C (Figure 3). We identified one overlapping QTL for stripe
606 ratio at both temperatures (Table 2). Based on the trait correlation and the shared QTL, at
607 least part of the genetic architecture underlying adaptive melanism appears to be shared
608 between temperatures.

609 The reaction norm of four pigmentation QTLs also showed that flies raised at 15 °C
610 showed darker phenotypes for all traits and even darker phenotypes for the Ethiopia
611 homozygotes, as expected (Figure 3). We also found significant genotype-by-environment
612 interactions for two of these QTLs – A4 Background and stripe ratio (Figure 3C-D). The
613 change in stripe ratio (Figure 3D) was greater for flies with the homozygous Ethiopia
614 genotype. Here, the more derived-like environment appears to enhance the phenotypic
615 consequences of the Ethiopian pigmentation variants. In contrast, for the A4 Background
616 QTL, the phenotype means at 15 °C only show a small difference between homozygous
617 genotypes, compared to the much larger difference at 25 °C, which is congruent with this

618 QTL being found only at 25 °C (whereas differences in the heterozygote means may reflect
619 small sample size effects).
620
621

622 **Discussion**

623 We report the creation of two new *Drosophila melanogaster* RIL panels established
624 from crosses between single inbred lines from Ethiopia and Zambia, and from France and
625 Zambia. We used these new data sets, together with an updated QTL mapping approach
626 focusing on additive effects, to investigate the genetic architectures of multiple traits that
627 have evolved become differentiated between *D. melanogaster* populations. We did not find
628 evidence for strong epistasis underlying their evolution, but genotype-by-environment
629 interactions were supported for two of the three traits investigated.
630

631 ***Genetic architectures underlying trait evolution***

632 Our QTL mapping results indicate genetic architectures for most traits involving
633 detectable loci with non-trivial effect sizes (5.3% to 21.4%; Table 2), consistent with past
634 bulk mapping studies for some of these traits (Bastide *et al.* 2016, Sprengelmeyer *et al.*
635 2020, Sprengelmeyer *et al.* 2021). In combination with those studies, our results reinforce
636 previous findings that evolved populations maintain persistent variability in the genetic
637 basis of pigmentation traits, wing length, and ethanol resistance. We did not find
638 significant QTLs for cold tolerance or thermal plasticity of pigmentation, which could
639 reflect either a more complex genetic basis of those traits or else greater non-genetic
640 variance in those assays.

641 We have also identified genes within the detected QTLs that might be underlying the
642 relevant traits, including genes previously known to be related to the phenotype and, with
643 the use of population genetic signatures of selection, novel candidate genes (Table 3). The
644 identified genes represent viable hypotheses for contributors to the genetic architecture of
645 traits that appear to have evolved due to local adaptation targeting either these or
646 pleiotropically correlated traits. Additional studies using functional approaches such as
647 genome editing will be needed to confirm the roles of these genes in the evolution of the
648 respective traits.

649

650 ***Lack of evidence for epistasis***

651 Despite the pervasiveness of epistasis underlying the genetic basis of complex traits
652 (Huang *et al.* 2012, Mackay 2014), we did not find evidence of epistasis involving any of the
653 detected adaptive loci (Table 2). In light of our power analysis (Figure 2), our empirical
654 results primarily argue against the presence of modifier variants within our RIL panels that
655 trigger sign epistasis, complete masking epistasis, or strong positive epistasis with regard
656 to the main effect loci. In contrast, our study does not speak to the presence of
657 quantitatively negative epistasis (*e.g.* diminishing returns epistasis) or more moderate
658 positive synergistic epistasis.

659 Previous studies have also found mixed results when investigating epistatic
660 interaction among adaptive loci (Malmberg & Mauricio 2005). In some cases, the varied
661 outcome for adaptive traits might reflect the transient nature of epistatic interactions in a
662 population, given that the epistatic effects of two loci on a trait depend on the allele
663 frequency of the interacting alleles. Interestingly, studies mapping QTLs for fitness-related

664 traits (more directly related to reproduction and survival) have a more consistent result,
665 often showing more epistatic QTLs than additive QTLs (Malmberg & Mauricio 2005).
666 One of the difficulties in extrapolating the results of experimental crosses to natural
667 populations is that experimental crosses start with a limited amount of genetic variation
668 (Mackay 2014). In our case, the crosses were made between one inbred line from each
669 parental population, which will exclude some variants present in the source populations
670 while elevating some naturally rare variants to moderate frequency. However, our crosses
671 have the advantage of focusing on a simplified genetic architecture, which may improve
672 power to detect interactions among the variants present, in addition to clear inference of
673 the parental origin of alleles genomewide.
674 We highlight that our study likely underestimates the epistatic interactions affecting
675 *D. melanogaster* adaptive traits, since we only had power to detect relative strong
676 interactions (Figure 2, Table S6). Based on the limited numbers of RILs available, we could
677 only detect strong additive QTLs, and we needed to focus our epistasis scan on interactions
678 with those few strong QTLs. Future research with a larger sample size (e.g. Torgeman &
679 Zamir 2023) would be helpful to achieve more extensive insights into the scope of epistatic
680 interactions affecting traits such as these.
681
682 ***Genetic Architectures at Two Temperatures***
683 Although the three body pigmentation traits we studied were somewhat correlated
684 (Table S3), no shared QTL was noted between them (Table 2). Instead, we found two
685 instances of overlapping or neighboring QTLs for the same trait measured at different
686 temperatures, with 25 °C and 15 °C being more similar to the mean temperatures in the
687 Zambian and Ethiopian populations, respectively. These results are compatible with the

688 same or nearby genes being responsible for pigmentation differences at both
689 temperatures.

690 *Drosophila* pigmentation is known to show thermal plasticity, and Ethiopian flies
691 would have been expected to become somewhat darken on this basis alone, and yet they
692 have also adapted genetically to become darker (Bastide *et al*. 2014). It is unclear whether
693 this pigmentation plasticity is adaptive, which in itself can facilitate adaptive evolution
694 (Ghalambor *et al*. 2007). Unlike larger ectotherms, it has been estimated that the solar gain
695 in temperature from having dark pigmentation is at most a fraction of a degree for an
696 organism with the small size and high surface to volume ratio of *Drosophila* (Willmer &
697 Unwin 1981, Hirai & Kimura 1997). Across African populations of *D. melanogaster*, levels
698 of ultraviolet radiation have been found to be stronger predictors of pigmentation than
699 temperature (Bastide *et al*. 2014).

700 Gene-by-environment loci have recently been shown to be enriched for signatures
701 of positive selection (Lea *et al*. 2022), supporting the hypothesis that environment-specific
702 loci play an important role in local adaptation. Here, we did find that two QTLs underlying
703 pigmentation evolution showed significant genotype-by-environment interactions (Figure
704 3), suggesting that the rate of their response to selective events might have changed upon
705 colonization of colder environments. However, we did not find consistent patterns of
706 either gene-by-gene or gene-by-environment interactions that met the predictions of
707 cryptic variation. For example, the absence of epistatic interactions means that the
708 Ethiopian alleles did not have their effect completely masked or reversed by another gene
709 on the ancestral background. And in the case of gene-environment interactions, there was
710 an enhanced QTL effect in the derived Ethiopia-like cool environment in just one of two

711 significant cases (*i.e.* the stripe QTL). While cryptic variation may have played a role in the
712 evolution of some or all of these traits, our results suggest that it may not have been
713 pervasive with respect to the strongest effect changes.
714
715 **Conclusion**
716 While the genetic architecture underlying adaptive evolution may vary somewhat
717 depending upon the trait, there remains a key interest in assessing potentially general
718 patterns. In combination with past studies, our results suggest that most adaptive trait
719 changes involve variants of non-trivial effect size, and that these variants often do not
720 initially reach fixation. Epistasis is an important component underlying complex traits,
721 including in flies (Huang *et al*. 2012), but we did not find evidence that strong epistasis was
722 relevant for the adaptive evolution of the studied loci. In light of the existence of other
723 examples in which epistasis among adaptive loci have been shown (Malmberg & Mauricio
724 2005), our study highlights that the answer to the classic debate on whether epistasis is
725 important to natural selection might vary case by case. Lastly, we found evidence of gene-
726 by-environment interactions underlying pigmentation, stressing that the variability of
727 genetic architectures can also be environment-dependent, which is particularly relevant in
728 light of rapidly changing global environments.
729
730 **Data availability**: Source code used in the analyses is available on GitHub
731 (https://github.com/ribeirots/RILepi). Raw sequence read data for the Recombinant
732 Inbred Lines are available on the Sequence Read Archive (BioProject: PRJNA861300).
733

Acknowledgments: We thank members of the Pool lab for helpful comments on this manuscript.

Conflict of interest: The authors declare no conflict of interest.

Funding: This research was funded by NIH grants R01 GM127480 and R35 GM136306.

References

Abramoff, M. D., Magalhães, P. J., & Ram, S. J. (2004). Image processing with ImageJ. Biophotonics International, 11(7), 36–42.

Adams, M., McBroome, J., Maurer, N., Pepper-Tunick, E., Saremi, N. F., Green, R. E., Vollmers, C., & Corbett-Detig, R. B. (2020). One fly–one genome: chromosome-scale genome assembly of a single outbred Drosophila melanogaster. Nucleic Acids Research, 48(13), e75-e75. doi:10.1093/nar/gkaa450.

Ang, R. M. L., Chen, S. A. A., Kern, A. F., Xie, Y., & Fraser, H. B. (2023). Widespread epistasis among beneficial genetic variants revealed by high-throughput genome editing. Cell Genomics, 3(4). doi:10.1016/j.xgen.2023.100260.

Arthur, B. J., Ding, Y., Sosale, M., Khalif, F., Kim, E., Waddell, P., Turaga, S. C., & Stern, D. L. (2021). SongExplorer: A deep learning workflow for discovery and segmentation of animal acoustic communication signals (p. 2021.03.26.437280). bioRxiv. doi:10.1101/2021.03.26.437280.

Arthur, B. J., Sunayama-Morita, T., Coen, P., Murthy, M., & Stern, D. L. (2013). Multi-channel acoustic recording and automated analysis of Drosophila courtship songs. BMC Biology, 11(1), 11. doi:10.1186/1741-7007-11-11.

Bank, C. (2022). Epistasis and adaptation on fitness landscapes. Annual Review of Ecology, Evolution, and Systematics, 53, 457-479. doi:10.1146/annurev-ecolsys-102320-112153.

Barton, N. H. (2017). How does epistasis influence the response to selection? Heredity, 118(1), 96-109. doi:10.1038/hdy.2016.109.

Bastide, H., Lange, J. D., Lack, J. B., Yassin, A., & Pool, J. E. (2016). A variable genetic architecture of melanic evolution in Drosophila melanogaster. Genetics, 204(3), 1307–1319. doi:10.1534/genetics.116.192492.

Bastide, H., Yassin, A., Johanning, E. J., & Pool, J. E. (2014). Pigmentation in Drosophila melanogaster reaches its maximum in Ethiopia and correlates most strongly with ultra-violet radiation in sub-Saharan Africa. BMC Evolutionary Biology, 14(1), 179. doi:10.1186/s12862-014-0179-y.

Bejarano, F., Luque, C. M., Herranz, H., Sorrosal, G., Rafel, N., Pham, T. T., & Milán, M. (2008). A gain-of-function suppressor screen for genes involved in dorsal–ventral boundary formation in the Drosophila wing. Genetics, 178(1), 307-323.. http://dx.doi.org/10.1534/genetics.107.081869.

Blanco, E., Ruiz-Romero, M., Beltran, S., Bosch, M., Punset, A., Serras, F., & Corominas, M. (2010). Gene expression following induction of regeneration in Drosophila wing

775 imaginal discs. Expression profile of regenerating wing discs. BMC Developmental
776 Biology, 10(1), 1-14. http://dx.doi.org/10.1186/1471-213X-10-94.

777 Broman, K. W., Wu, H., Sen, Ś., & Churchill, G. A. (2003). R/qtl: QTL mapping in experimental
778 crosses. Bioinformatics, 19(7), 889–890. doi:10.1093/bioinformatics/btg112.

779 Carter, A. J., Hermisson, J., & Hansen, T. F. (2005). The role of epistatic gene interactions in
780 the response to selection and the evolution of evolvability. Theoretical Population
781 Biology, 68(3), 179-196. doi:10.1016/j.tpb.2005.05.002.

782 Clemens, J., Coen, P., Roemschied, F. A., Pereira, T. D., Mazumder, D., Aldarondo, D. E.,
783 Pacheco, D. A., & Murthy, M. (2018). Discovery of a new song mode in Drosophila reveals
784 hidden structure in the sensory and neural drivers of behavior. Current Biology, 28(15),
785 2400-2412.e6. doi:10.1016/j.cub.2018.06.011.

786 Cohan, F. M., & Graf, J.-D. (1985). Latitudinal cline in Drosophila melanogaster for
787 knockdown resistance to ethanol fumes and for rates of response to selection for
788 further resistance. Evolution, 39(2), 278–293. doi:10.2307/2408362.

789 Comeron, J. M., Ratnappan, R., & Bailin, S. (2012). The many landscapes of recombination in
790 Drosophila melanogaster. PLOS Genetics, 8(10), e1002905.
791 doi:10.1371/journal.pgen.1002905.

792 Crow, J. F. (2010). On epistasis: why it is unimportant in polygenic directional selection.
793 Philosophical Transactions of the Royal Society B: Biological Sciences, 365(1544),
794 1241–1244. doi:10.1098/rstb.2009.0275.

795 da Silva Ribeiro, T., Galván, J. A., & Pool, J. E. (2022). Maximum SNP FST outperforms full-
796 window statistics for detecting soft sweeps in local adaptation. Genome Biology and
797 Evolution, 14(10), evac143. doi:10.1093/gbe/evac143.

798 David, J. R., Capy, P., & Gauthier, J.-P. (1990). Abdominal pigmentation and growth
799 temperature in Drosophila melanogaster: similarities and differences in the norms of
800 reaction of successive segments. Journal of Evolutionary Biology, 3(5–6), 429–445.
801 doi:10.1046/j.1420-9101.1990.3050429.x.

802 Dewey, E. M., McNabb, S. L., Ewer, J., Kuo, G. R., Takanishi, C. L., Truman, J. W., & Honegger, H.
803 W. (2004). Identification of the gene encoding bursicon, an insect neuropeptide
804 responsible for cuticle sclerotization and wing spreading. Current Biology, 14(13),
805 1208-1213.. http://dx.doi.org/10.1016/j.cub.2004.06.051.

806 Doust, A. N., Lukens, L., Olsen, K. M., Mauro-Herrera, M., Meyer, A., & Rogers, K. (2014).
807 Beyond the single gene: How epistasis and gene-by-environment effects influence crop
808 domestication. Proceedings of the National Academy of Sciences, 111(17), 6178-6183.
809 doi:10.1073/pnas.1308940110.

Duchêne, E., Butterlin, G., Dumas, V., & Merdinoglu, D. (2012). Towards the adaptation of grapevine varieties to climate change: QTLs and candidate genes for developmental stages. Theoretical and Applied Genetics, 124(4), 623-635. doi:10.1007/s00122-011-1734-1.

Dworkin, I., & Gibson, G. (2006). Epidermal growth factor receptor and transforming growth factor-β signaling contributes to variation for wing shape in Drosophila melanogaster. Genetics, 173(3), 1417-1431. http://dx.doi.org/10.1534/genetics.105.053868.

Fenster, C. B., Galloway, L. F., & Chao, L. (1997). Epistasis and its consequences for the evolution of natural populations. Trends in Ecology & Evolution, 12(7), 282–286. doi:10.1016/S0169-5347(97)81027-0.

Fisher, R. A. (1930). The genetical theory of natural selection (pp. xiv, 272). Clarendon Press. doi:10.5962/bhl.title.27468.

Flynn, J. M., Rossouw, A., Cote-Hammarlof, P., Fragata, I., Mavor, D., Hollins III, C., Bank, C., & Bolon, D. N. (2020). Comprehensive fitness maps of Hsp90 show widespread environmental dependence. Elife, 9, e53810. doi:10.7554/eLife.53810.

Fochler, S., Morozova, T. V., Davis, M. R., Gearhart, A. W., Huang, W., Mackay, T. F., & Anholt, R. R. (2017). Genetics of alcohol consumption in Drosophila melanogaster. Genes, Brain and Behavior, 16(7), 675-685. doi:10.1111/gbb.12399.

Fry, J. D., Nuzhdin, S. V., Pasyukova, E. G., & Mackay, T. F. (1998). QTL mapping of genotype–environment interaction for fitness in Drosophila melanogaster. Genetics Research, 71(2), 133-141. doi:10.1017/S0016672398003176.

Fuhrmann, N., Prakash, C., & Kaiser, T. S. (2023). Polygenic adaptation from standing genetic variation allows rapid ecotype formation. Elife, 12, e82824. doi:10.7554/eLife.82824.

Ghalambor, C. K., McKay, J. K., Carroll, S. P., & Reznick, D. N. (2007). Adaptive versus non-adaptive phenotypic plasticity and the potential for contemporary adaptation in new environments. Functional Ecology, 21(3), 394–407. doi:10.1111/j.1365-2435.2007.01283.x.

Gibson, G., & Dworkin, I. (2004). Uncovering cryptic genetic variation. Nature Reviews Genetics 5, 681–690. doi:10.1038/nrg1426.

Gong, L. I., & Bloom, J. D. (2014). Epistatically interacting substitutions are enriched during adaptive protein evolution. PLoS Genetics, 10(5). doi:10.1371/journal.pgen.1004328.

Griswold, C. (2006). Gene flow's effect on the genetic architecture of a local adaptation and its consequences for QTL analyses. Heredity, 96, 445-453. doi:10.1038/sj.hdy.6800822.

Hansen, T. F., Álvarez-Castro, J. M., Carter, A. J., Hermisson, J., & Wagner, G. P. (2006). Evolution of genetic architecture under directional selection. Evolution, 60(8), 1523-1536. doi:10.1111/j.0014-3820.2006.tb00498.x.

Hansen, T. F. (2013). Why epistasis is important for selection and adaptation. Evolution, 67(12), 3501–3511. doi:10.1111/evo.12214.

Hill, W. G., Goddard, M. E., & Visscher, P. M. (2008). Data and theory point to mainly additive genetic variance for complex traits. PLOS Genetics, 4(2), e1000008. doi:10.1371/journal.pgen.1000008.

Hirai, Y., & Kimura, M. T. (1997). Incipient reproductive isolation between two morphs of Drosophila elegans (Diptera: Drosophilidae). Biological Journal of the Linnean Society, 61(4), 501-513. doi:10.1111/j.1095-8312.1997.tb01804.x.

Huang, W., Carbone, M. A., Lyman, R. F., Anholt, R. R., & Mackay, T. F. (2020). Genotype by environment interaction for gene expression in Drosophila melanogaster. Nature Communications, 11(1), 5451. doi:10.1038/s41467-020-19131-y.

Huang, Y., Lack, J. B., Hoppel, G. T., & Pool, J. E. (2021). Parallel and population-specific gene regulatory evolution in cold-adapted fly populations. Genetics, 218(3). doi:10.1093/genetics/iyab077.

Huang, W., Richards, S., Carbone, M. A., Zhu, D., Anholt, R. R. H., Ayroles, J. F., Duncan, L., Jordan, K. W., Lawrence, F., Magwire, M. M., Warner, C. B., Blankenburg, K., Han, Y., Javaid, M., Jayaseelan, J., Jhangiani, S. N., Muzny, D., Ongeri, F., Perales, L., … Mackay, T. F. C. (2012). Epistasis dominates the genetic architecture of Drosophila quantitative traits. Proceedings of the National Academy of Sciences, 109(39), 15553–15559. doi:10.1073/pnas.1213423109.

Juenger, T. E., Sen, S., Stowe, K. A., & Simms, E. L. (2005). Epistasis and genotype-environment interaction for quantitative trait loci affecting flowering time in Arabidopsis thaliana. Genetica, 123, 87-105. doi:10.1007/s10709-003-2717-1.

Krishnan, S. N., Frei, E., Swain, G. P., & Wyman, R. J. (1993). Passover: a gene required for synaptic connectivity in the giant fiber system of Drosophila. Cell, 73(5), 967-977. doi:10.1016/0092-8674(93)90274-T.

Krupp, J. J., Yaich, L. E., Wessells, R. J., & Bodmer, R. (2005). Identification of genetic loci that interact with cut during Drosophila wing-margin development. Genetics, 170(4), 1775-1795. http://dx.doi.org/10.1534/genetics.105.043125.

Lachaise, D., Cariou, M.-L., David, J. R., Lemeunier, F., Tsacas, L., & Ashburner, M. (1988). Historical biogeography of the Drosophila melanogaster species subgroup. In M. K. Hecht, B. Wallace, & G. T. Prance (Eds.), Evolutionary Biology (pp. 159–225). Springer US. doi:10.1007/978-1-4613-0931-4_4.

880 Lack, J. B., Cardeno, C. M., Crepeau, M. W., Taylor, W., Corbett-Detig, R. B., Stevens, K. A.,
881 Langley, C. H., & Pool, J. E. (2015). The Drosophila genome nexus: a population genomic
882 resource of 623 Drosophila melanogaster genomes, including 197 from a single
883 ancestral range population. Genetics, 199(4), 1229–1241.
884 doi:10.1534/genetics.115.174664.

885 Lack, J. B., Monette, M. J., Johanning, E. J., Sprengelmeyer, Q. D., & Pool, J. E. (2016).
886 Decanalization of wing development accompanied the evolution of large wings in high-
887 altitude Drosophila. Proceedings of the National Academy of Sciences, 113(4), 1014–
888 1019. doi:10.1073/pnas.1515964113.

889 Lande, R. 1992. Neutral theory of quantitative genetic variance in an island model with local
890 extinction and colonization. Evolution, 46:381–389. doi:10.1111/j.1558-
891 5646.1992.tb02046.x.

892 Lange, J. D., & Pool, J. E. (2016). A haplotype method detects diverse scenarios of local
893 adaptation from genomic sequence variation. Molecular Ecology, 25(13), 3081-3100.
894 doi:10.1111/mec.13671.

895 Lea, A. J., Peng, J., & Ayroles, J. F. (2022). Diverse environmental perturbations reveal the
896 evolution and context-dependency of genetic effects on gene expression levels. Genome
897 Research, 32(10), 1826-
898 1839.https://www.genome.org/cgi/doi/10.1101/gr.276430.121.

899 Li, H. (2013). Aligning sequence reads, clone sequences and assembly contigs with BWA-
900 MEM. arXiv:1303.3997 [q-Bio]. http://arxiv.org/abs/1303.3997.

901 Lollar, M. J., da Silva Ribeiro, T., Stern. D., & Pool, J. E. (2024in Prep). Quantitative trait
902 mapping of courtship song variation between male Drosophila melanogaster from two
903 allopatric populations. biorxiv, 2024-05.

904 López-Varea, A., Vega-Cuesta, P., Ruiz-Gómez, A., Ostalé, C. M., Molnar, C., Hevia, C. F., Martín,
905 M., Organista, M. F., de Celis, J., Culí, J., Esteban, N., & de Celis, J. F. (2021). Genome-wide
906 phenotypic RNAi screen in the Drosophila wing: Phenotypic description of functional
907 classes. G3, 11(12), jkab349. doi:10.1093/g3journal/jkab349.

908 Lowry, D. B., Lovell, J. T., Zhang, L., Bonnette, J., Fay, P. A., Mitchell, R. B., Lloyd-Reilley, J., Boe,
909 A. R., Wu, Y., Rouquette Jr, F. M., Wynia, R. L., Weng, X., Behrman, K. D., Healey, A., Barry,
910 K., Lipzen, A., Bauer, D., Sharma, A., Jenkins, J., Schmutz, J., Fritschi, F. B., & Juenger, T. E.
911 (2019). QTL × environment interactions underlie adaptive divergence in switchgrass
912 across a large latitudinal gradient. Proceedings of the National Academy of Sciences,
913 116(26), 12933-12941. doi:10.1073/pnas.1821543116.

914 Lunzer, M., Golding, G. B., & Dean, A. M. (2010). Pervasive cryptic epistasis in molecular
915 evolution. PLoS Genetics, 6(10). doi:10.1371/journal.pgen.1001162.

916 Lynch, M., & Walsh, B. (1998). Genetics and analysis of quantitative traits. Sinauer.

Mackay, T. F. (2001). The genetic architecture of quantitative traits. Annual Review of Genetics, 35(1), 303-339. doi:10.1146/annurev.genet.35.102401.090633.

Mackay, T. F. C. (2014). Epistasis and quantitative traits: Using model organisms to study gene–gene interactions. Nature Reviews Genetics, 15(1), 22–33. doi:10.1038/nrg3627.

Malmberg, R. L., & Mauricio, R. (2005). QTL-based evidence for the role of epistasis in evolution. Genetics Research, 86(2), 89–95. doi:10.1017/S0016672305007780.

Martin, G., & Lenormand, T. (2006). The fitness effect of mutations across environments: A survey in light of fitness landscape models. Evolution, 60(12), 2413-2427. doi:10.1111/j.0014-3820.2006.tb01878.x.

Massey, J. H., & Wittkopp, P. J. (2016). The genetic basis of pigmentation differences within and between Drosophila species. Current Topics in developmental Biology, 119, 27-61. doi:10.1016/bs.ctdb.2016.03.004.

Mathews, K. L., Malosetti, M., Chapman, S., McIntyre, L., Reynolds, M., Shorter, R., & Van Eeuwijk, F. (2008). Multi-environment QTL mixed models for drought stress adaptation in wheat. Theoretical and Applied Genetics, 117, 1077-1091. doi:10.1007/s00122-008-0846-8.

McGuigan, K., & Sgro, C. M. (2009). Evolutionary consequences of cryptic genetic variation. Trends in Ecology & Evolution, 24(6), 305-311. doi:10.1016/j.tree.2009.02.001.

Okada, H., Ebhardt, H. A., Vonesch, S. C., Aebersold, R., & Hafen, E. (2016). Proteome-wide association studies identify biochemical modules associated with a wing-size phenotype in Drosophila melanogaster. Nature Communications, 7(1), 12649. http://dx.doi.org/10.1038/ncomms12649.

Orr, H. A. (1998). The population genetics of adaptation: the distribution of factors fixed during adaptive evolution. Evolution, 52(4), 935–949. doi:10.1111/j.1558-5646.1998.tb01823.x.

Papa, R., Kapan, D. D., Counterman, B. A., Maldonado, K., Lindstrom, D. P., Reed, R. D., Nijhout, H. F., Hrbek, T., & McMillan, W. O. (2013). Multi-allelic major effect genes interact with minor effect QTLs to control adaptive color pattern variation in Heliconius erato. PLoS One, 8(3), e57033. doi:10.1371/journal.pone.0057033.

Parker, J., & Struhl, G. (2015). Scaling the Drosophila wing: TOR-dependent target gene access by the Hippo pathway transducer Yorkie. PLoS Biology, 13(10), e1002274.. http://dx.doi.org/10.1371/journal.pbio.1002274.

Paul, L., Wang, S. H., Manivannan, S. N., Bonanno, L., Lewis, S., Austin, C. L., & Simcox, A. (2013). Dpp-induced Egfr signaling triggers postembryonic wing development in Drosophila. Proceedings of the National Academy of Sciences, 110(13), 5058-5063. http://dx.doi.org/10.1073/pnas.1217538110.

953 Pitchers, W., Pool, J. E., & Dworkin, I. (2013). Altitudinal clinal variation in wing size and
954 shape in African Drosophila melanogaster: one cline or many? Evolution, 67(2), 438–
955 452. doi:10.1111/j.1558-5646.2012.01774.x.

956 Pool, J. E. (2015). The mosaic ancestry of the Drosophila Genetic Reference Panel and the D.
957 melanogaster reference genome reveals a network of epistatic fitness interactions.
958 Molecular Biology and Evolution, 32(12), 3236–3251. doi:10.1093/molbev/msv194.

959 Pool, J. E., & Aquadro, C. F. (2006). History and structure of sub-Saharan populations of
960 Drosophila melanogaster. Genetics, 174(2), 915–929.
961 doi:10.1534/genetics.106.058693.

962 Pool, J. E., Braun, D. T., & Lack, J. B. (2017). Parallel evolution of cold tolerance within
963 Drosophila melanogaster. Molecular Biology and Evolution, 34(2), 349–360.
964 doi:10.1093/molbev/msw232.

965 Pritchard, J. K., Pickrell, J. K., & Coop, G. (2010). The genetics of human adaptation: hard
966 sweeps, soft sweeps, and polygenic adaptation. Current Biology, 20(4), R208-R215.
967 doi:10.1016/j.cub.2009.11.055.

968 Reynolds, J., Weir, B. S., & Cockerham, C. C. (1983). Estimation of the coancestry coefficient:
969 basis for a short-term genetic distance. Genetics, 105(3), 767-779.
970 doi:10.1093/genetics/105.3.767.

971 Rogers, W. A., Grover, S., Stringer, S. J., Parks, J., Rebeiz, M., & Williams, T. M. (2014). A survey
972 of the trans-regulatory landscape for Drosophila melanogaster abdominal pigmentation.
973 Developmental Biology, 385(2), 417-432. doi:10.1016/j.ydbio.2013.11.013.

974 Rutherford, S. L., & Lindquist, S. (1998). Hsp90 as a capacitor for morphological evolution.
975 Nature, 396(6709), 336-342. doi:10.1038/24550.

976 Savolainen, O., Lascoux, M., & Merilä, J. (2013). Ecological genomics of local adaptation.
977 Nature Reviews Genetics, 14, 807-820. doi:10.1038/nrg3522.

978 Schertel, C., Albarca, M., Rockel-Bauer, C., Kelley, N. W., Bischof, J., Hens, K., van Nimwegen,
979 E., Basier, K., & Deplancke, B. (2015). A large-scale, in vivo transcription factor screen
980 defines bivalent chromatin as a key property of regulatory factors mediating Drosophila
981 wing development. Genome Research, 25(4), 514-523. doi:10.1101/gr.181305.114.

982 Schlötterer, C. (2023). How predictable is adaptation from standing genetic variation?
983 Experimental evolution in Drosophila highlights the central role of redundancy and
984 linkage disequilibrium. Philosophical Transactions of the Royal Society B, 378(1877),
985 20220046. doi:10.1098/rstb.2022.0046.

986 Spitze, K. 1993. Population structure in Daphnia obtusa: quantitative genetic and allozymic
987 variation. Genetics. 135:367–374. doi:10.1093/genetics/135.2.367

Sprengelmeyer, Q. D., Mansourian, S., Lange, J. D., Matute, D. R., Cooper, B. S., Jirle, E. V., Stensmyr, M. C., & Pool, J. E. (2020). Recurrent collection of Drosophila melanogaster from wild African environments and genomic insights into species history. Molecular Biology and Evolution, 37(3), 627–638. doi:10.1093/molbev/msz271.

Sprengelmeyer, Q. D., & Pool, J. E. (2021). Ethanol resistance in Drosophila melanogaster has increased in parallel cold-adapted populations and shows a variable genetic architecture within and between populations. Ecology and Evolution, 11(21), 15364–15376. doi:10.1002/ece3.8228.

Starr, T. N., & Thornton, J. W. (2016). Epistasis in protein evolution. Protein Science, 25(7), 1204-1218. doi:10.1002/pro.2897.

Steiner, C. C., Weber, J. N., & Hoekstra, H. E. (2007). Adaptive variation in beach mice produced by two interacting pigmentation genes. PLoS Biology, 5(9), e219. doi:10.1371/journal.pbio.0050219.

Stitzer, M. C., & Ross-Ibarra, J. (2018). Maize domestication and gene interaction. New Phytologist, 220(2), 395-408. doi:10.1111/nph.15350.

Torgeman, S., & Zamir, D. (2023). Epistatic QTLs for yield heterosis in tomato. Proceedings of the National Academy of Sciences, 120(14), e2205787119. doi:10.1073/pnas.2205787119.

Trindade, S., Sousa, A., Xavier, K. B., Dionisio, F., Ferreira, M. G., & Gordo, I. (2009). Positive epistasis drives the acquisition of multidrug resistance. PLOS Genetics, 5(7), e1000578. doi:10.1371/journal.pgen.1000578.

Van Rossum, G., & Drake, F. L. (2009). Python 3 Reference Manual. Scotts Valley, CA: CreateSpace.

Vijendravarma, R. K., & Kawecki, T. J. (2013). Epistasis and maternal effects in experimental adaptation to chronic nutritional stress in Drosophila. Journal of Evolutionary Biology, 26(12), 2566-2580. doi:10.1111/jeb.12248.

Wade, M. J. (1992). Sewall Wright: Gene interaction and the shifting balance theory. In Oxford surveys in evolutionary biology (Vol. 8, pp. 35–35).

Whitlock, M. C., Phillips, P. C., Moore, F. B.-G., & Tonsor, S. J. (1995). Multiple fitness peaks and epistasis. Annual Review of Ecology and Systematics, 26(1), 601–629. doi:10.1146/annurev.es.26.110195.003125.

Willmer, P. G., & Unwin, D. M. (1981). Field analyses of insect heat budgets: reflectance, size and heating rates. Oecologia, 50, 250-255. doi:10.1007/BF00348047.

Wright, S. (1931). Evolution in Mendelian populations. Genetics, 16(2), 97–159. doi:10.1093%2Fgenetics%2F16.2.97.

1023 Yeaman, S. & Otto, S. P. (2011). Establishment and maintenance of adaptive genetic
1024 divergence under migration, selection, and drift. Evolution, 65(7), 2123–2129.
1025 doi:10.1111/j.1558-5646.2011.01277.x.

1026 Yeaman, S., & Whitlock, M. C. (2011). The genetic architecture of adaptation under
1027 migration-selection balance. Evolution, 65(7), 1897–1911. doi:10.1111/j.1558-
1028 5646.2011.01269.x.

1029 Yukilevich, R., Lachance, J., Aoki, F., & True, J. R. (2008). Long-term adaptation of epistatic
1030 genetic networks. Evolution, 62(9), 2215-2235. doi:10.1111/j.1558-
1031 5646.2008.00445.x.

1032 Zeng, Z. B., Kao, C. H., & Basten, C. J. (1999). Estimating the genetic architecture of
1033 quantitative traits. Genetics Research, 74(3), 279-289.
1034 doi:10.1017/S0016672399004255.

1035 Zheng, Y., Liu, B., Wang, L., Lei, H., Prieto, K. D. P., & Pan, D. (2017). Homeostatic control of
1036 Hpo/MST kinase activity through autophosphorylation-dependent recruitment of the
1037 STRIPAK PP2A phosphatase complex. Cell Reports, 21(12), 3612-3623.
1038 doi:10.1016/j.celrep.2017.11.076.